Mathematics and Computation, Supercomputing, Reactor Physics and Nuclear and Biological Applications
Palais des Papes, Avignon, France, September 12-15, 2005, on CD-ROM, American Nuclear Society, LaGrange Park, IL (2005)

MULTIPLE TIME-SCALE APPROXIMATIONS FOR THE TIME DEPENDENT P_1 AND P_3 EQUATIONS

Bruno Merk
Institut für Reaktorsicherheit
Forschungszentrum Karlsruhe
Postfach 3640, D-76021 Karlsruhe
merk@irs.fzk.de

Dan G. Cacuci
Institut für Kerntechnik und Reaktorsicherheit
Universität Karlsruhe
Haid-und-Neu-Str. 7, Postbox Nr. 45, D-76131 Karlsruhe
cacuci@ikr.uni-karlsruhe.de

ABSTRACT

This work presents the derivation of a closed form expression as well for a three time-scales approximation of the point kinetics equations, as the one-group time-dependent P_1- and P_3-equations, for a homogeneous multiplying medium, in planar geometry. The results produced by the three-scale approximation for the point kinetics equations are shown to be practically as accurate as the numerical results produced by the Kaganove-type algorithms used in production codes, yet at significantly less costs in computational time and resources. For the P1 equations, closed-form three-scale approximations have been derived for the neutron flux and its higher-order spherical harmonics, as well as for the precursors for two groups of delayed neutrons. The development of these three-scale approximations did not rely on imposing separation of space and time; furthermore, they offer the possibility of a direct investigation of the differences between the P_1-, P_3-, and diffusion equations, respectively. In particular, significant differences are observed regarding the time-behavior of the various approximations for the neutron current, smaller differences are observed regarding the differences in the time-behavior of the various expressions for the neutron flux, while the distinctions between the various approximations for the precursor distributions are negligible. Furthermore, the three-scale approximations for the P_1- and P_3-equations have been shown to be superior to the results offered by the improved quasistatic methods described in the literature, particularly for the shortest time scales in the presence of large reactivity insertions.
In summary, the method of multiple-scale expansion offers a new way for developing very accurate and effective approximations for solving typical stiff-systems, such as the time-dependent neutron transport and/or diffusion equations with delayed neutrons.

KEYWORDS: Multiple-Scale Expansion, Reactor Kinetics, P_N-Equations

1. INTRODUCTION

As is well known, the transient behavior of a nuclear system is governed by the distinct time scales of the prompt and delayed neutron production. Thus, a reliable computation of the transient local power distribution within the reactor's core would require the solution of the space-, time-, energy- and angle-dependent neutron transport equation with delayed neutrons. In practice, however, it is not feasible to solve exactly the time-dependent neutron transport equation for realistic reactor core geometries, because of the tremendous requirements in computer power and memory demand. Popular approximations include the synthesis and space-time separation methods [1], finite difference methods [2], modal expansion methods [3], the quasi-static method [4], the point reactor model [5], and coarse mesh [6,7] or nodal methods [8]. The standard methods for simulating the neutron kinetics behavior of light water reactors (LWR) rely on solving the time dependent neutron diffusion equation, without space-time separation, using coarse mesh or nodal methods. For fast reactor systems, however, the neutron generation time is about 1000 times smaller than for a light water reactor. Consequently, direct discretization of the time derivative term in the transport or diffusion equation (as used for LWR's) would lead to prohibitively long computational time and memory demands, because the computational time-step size is dictated by the neutron generation time. The today's standard for fast reactor calculations are the quasi-static method [9] or the point kinetics method [10,11]. However, the separation of space and time within these methods is in some cases insufficiently accurate.
The distinct time scales for generation of the prompt and delayed neutrons cause the systems of equations produced by any of the above approximations to display a stiff behavior in time. For such stiff systems, regular perturbation methods fail to predict accurately the reactor's long-time behavior because of the inevitable accumulation of the overall errors, which grow in time even if the local errors, at every time step, are small. On the other hand, the existence of clearly separated time scales suggests the use of a multiple-scale expansion [12,13] for deriving solutions that retain their asymptotic validity, for large time values. The distinct time-scales for such expansions are given by the time scales of the prompt and delayed neutron production.
The objective of this work is to apply the method of multiple-scales expansion to develop efficient analytical approximations for describing the time behavior of the neutron population and the precursor concentration in a multiplying system with delayed neutrons. As will be shown, the time-step in the approximation functions is independent of the neutron generation time. Therefore, large time-steps can be used, without adversely affecting the solution's accuracy.
The principles of applying the multiple-scales expansion method are demonstrated in Section 2 by using the point kinetics equations. The usability, accuracy and efficiency of the multiple time-scales equations obtained for computing the time behavior of the neutron population are discussed in Section 3. Also presented in this Section are results from several illustrative computations using the three-scale approximation for the P_1 and P_3 equations, for an idealized homogeneous slab reactor. Significant differences are observed regarding the time-behavior of the various approximations for the neutron current, smaller differences are observed regarding the differences in the time-behavior of the various expressions for the neutron flux, while the distinctions for the precursor distributions are negligible. Furthermore, the three-scale approximations for the P_1- and P_3-equations are shown to be superior to the improved quasistatic solutions described in the literature, particularly for the shortest time scales, in the presence of large reactivity insertions. The three-scale approximation (with two groups of delayed neutrons) for time-dependent P_1 is developed in the appendix.

2. THREE TIME-SCALES EXPANSIONS FOR THE POINT KINETICS EQUATION

The basic concepts and the practical application of the method of multiple scale expansion will be illustrated in this section by using the point kinetics equations for a multiplying system with delayed neutron production. Although the point kinetics equations represent a drastic simplification of the Boltzmann equation, they do possess the typical stiff behavior introduced by the delayed neutrons. The multiplicity of time-scales will be treated by using of the multiple scale expansion method.

The development of the multiple time-scales equations will commence by considering the point kinetics equations with n = 2 groups of delayed neutrons, which can be written in standard form as:

$$\frac{dn}{dt} = \frac{r-b}{\Lambda} n(t) + \sum_{m=1}^{n} l_m c_m(t) \tag{1}$$

$$\frac{dc_m}{dt} = \frac{b_m}{\Lambda} n(t) - l_m c_m(t), \quad m = 1, \mathbf{K}, n. \tag{2}$$

In the above equations, t denotes the time variable; $n(t)$ denotes the time-dependent population of neutrons, with effective life-time Λ; $c_m(t)$ represents the time-dependent concentration of the m^{th}-precursor, with decay constant λ_m and fraction β_m; ρ represents the reactivity of the system;

$b \equiv \sum_{m=1}^{n} b_m$; and n denotes the total number of groups of precursors.

To illustrate the separation of time-scales, the point kinetics equations Eq. 1 and Eq. 2 are recast in the following non-dimensional form:

$$\frac{dn}{dt} - an = e_1 c_1 + e_2 c_2 \tag{3}$$

$$\frac{dc_m}{dt} = b_m n - e_m c_m \qquad m = 1,2. \tag{4}$$

The following definitions have been used in the above equations:

$$a \equiv r - b \tag{5}$$

$$t \equiv \frac{t}{\Lambda} \tag{6}$$

$$e_m = l_m \Lambda, \qquad m = 1,2. \tag{7}$$

The distinct time scales involved implicitly in Eq. 1 and Eq. 2 can be identified in terms of the dimensionless time parameter τ and the "small parameters" ε_m, by expanding the dimensionless time parameter into the three time scales τ_0, τ_1 and τ_2, defined as follows:

$$t_0 \equiv t, \quad t_1 \equiv e_1 t, \quad t_2 \equiv e_2 t \tag{8}$$

Accordingly, the dependent variables n and c_m are considered to be functions of the three time scales, namely:

$$n = n(t_0, t_1, t_2), \tag{9}$$

$$c_m = c_m(t_0, t_1, t_2), \qquad m = 1, 2. \tag{10}$$

The time derivative operator is also expanded in the three time scales τ_0, τ_1 and τ_2:

$$\frac{d}{dt} = \sum_{i=0}^{n} \frac{dt_i}{dt} \frac{\partial}{\partial t_i} = \frac{\partial}{\partial t_0} + e_1 \frac{\partial}{\partial t_1} + e_2 \frac{\partial}{\partial t_2} + \mathbf{K} \tag{11}$$

In view of the above expansion it follows that the neutron population n and the precursor concentration c_m can be expanded formally in infinite series of the forms

$$n = n_0 + e_1 n_1 + e_2 n_2 + e_1^2 n_3 + \mathbf{K} \tag{12}$$

$$c_m = c_{m0} + e_1 c_{m1} + e_2 c_{m2} + e_1^2 c_{m3} + \mathbf{K} \qquad m = 1, 2. \tag{13}$$

Even though the accuracy of the approximations shown in Eq. 12 and Eq. 13 increases, in general, as more and more terms are retained in the respective expansions, it is important to note that while the accuracy of the single-scale expansions is usually improved by retaining higher-order terms in the respective expansion, the accuracy of multiple-scale expansions can be improved only if additional multi-scale information becomes available.

The multiple-scale equations are obtained by inserting Eq. 11, Eq. 12 and Eq. 13 into the dimensionless point kinetics equations Eq. 3 and Eq. 4, and subsequently collecting the terms that contain the same powers of ε. Thus, collecting the terms corresponding to e to the zeroth-(lowest-) power yields the following equations for the neutron population n_0 and the precursor concentrations c_{m0}:

$$\frac{\partial n_0}{\partial t_0} - a n_0 = 0 \tag{14}$$

,

$$\frac{\partial c_{m0}}{\partial t_0} = b_m n_0; \qquad m = 1, 2. \tag{15}$$

The system of first-order coupled ordinary differential equations represented by Eq. 14 and Eq. 15 provides information regarding the system's behavior on the fastest time scale, of the order of the prompt neutron generation time. This system can be readily solved to obtain the following closed-form solutions:

$$n_0 = A_0 e^{a t_0} \tag{16}$$

$$c_{10} = B_{10} + \frac{b_1}{a} A_0 e^{a t_0} \tag{17}$$

$$c_{20} = B_{20} + \frac{b_2}{a} A_0 e^{a t_0} \tag{18}$$

The above solutions contain time-dependent exponential functions and the yet undetermined coefficients A_0, B_{10}, and B_{20}, which can only be determined with help of the solutions to the higher-order equations of e. These coefficients provide information regarding the influence of the delayed neutron production on the short-time scale of the prompt neutron generation.

Collecting the coefficients of the first order of the expansion in e yields the following equations for neutron distributions n_1 and n_2, and the precursor concentrations c_{m1} and c_{m2}:

$$e_1 \frac{\partial n_1}{\partial t_0} + e_2 \frac{\partial n_2}{\partial t_0} + e_1 \frac{\partial n_0}{\partial t_1} + e_2 \frac{\partial n_0}{\partial t_2} - e_1 a n_1 - e_2 a n_2 = e_1 c_{10} + e_2 c_{20}, \tag{19}$$

$$e_1 \frac{\partial c_{m1}}{\partial t_0} + e_2 \frac{\partial c_{m2}}{\partial t_0} + e_1 \frac{\partial c_{m0}}{\partial t_1} + e_2 \frac{\partial c_{m0}}{\partial t_2} = e_1 b_m n_1 + e_2 b_m n_2 - e_m c_{m0}, \qquad m = 1, 2. \tag{20}$$

The above system of three coupled equations is characterized by the longer time scales associated with the production of delayed neutrons. To solve these equations, we use Eq. 16 through Eq. 18 in Eq. 19 and Eq. 20. The result is the following equation for the neutron distributions n_1 and n_2:

$$e_1\frac{\partial n_1}{\partial t_0}+e_2\frac{\partial n_2}{\partial t_0}-e_1an_1-e_2an_2=e_1B_{10}+e_1\frac{b_1}{a}A_0e^{at_0}+e_2B_{20}+e_2\frac{b_2}{a}A_0e^{at_0}-e_1\frac{\partial A_0}{\partial t_1}e^{at_0}-e_2\frac{\partial A_0}{\partial t_2}e^{at_0} \tag{21}$$

The above equation must be independent of any terms in τ_0, since the later are zero-order terms. Requiring, therefore, the vanishing of all terms in τ_0 leads to the following equation for the quantity A_0:

$$e_1\left(\frac{\partial A_0}{\partial t_1}-\frac{b_1}{a}A_0\right)+e_2\left(\frac{\partial A_0}{\partial t_2}-\frac{b_2}{a}A_0\right)=0 \tag{22}$$

The above equation can be readily solved to obtain

$$A_0(t_1,t_2)=D_0e^{\frac{b_1}{a}t_1+\frac{b_2}{a}t_2} \tag{23}$$

The quantity A_0 introduces the influence of the delayed neutron production into the equations for the short time horizon of the prompt neutron production. Note that the coefficient D_0 is a bone-fide constant, which would remain to be determined later, by using the initial conditions. Inserting now Eq. 22 into Eq. 21 simplifies the latter considerably, and the resulting first order differential equations for n_1 and n_2 can be solved to obtain

$$n_1=A_1e^{at_0}-\frac{1}{a}B_{10}, \tag{24}$$

$$n_2=A_2e^{at_0}-\frac{1}{a}B_{20}. \tag{25}$$

In the above equations, the coefficients A_1, A_2, B_{10} and B_{20} must be independent of t_0. Their expressions can be determined by using Eq. 16 trough Eq. 18, Eq. 24, and Eq. 25 in Eq. 20. The arising equations for the precursor concentrations c_{m1} and c_{m2} give the requirements for the coefficients B_{10} and B_{20}. This requirement is fulfilled by imposing the conditions:

$$e_1\frac{\partial B_{10}}{\partial t_1}+e_2\frac{\partial B_{10}}{\partial t_2}+e_1a_1B_{10}+e_1B_{10}=-e_2a_1B_{20} \tag{26}$$

$$e_1\frac{\partial B_{20}}{\partial t_1}+e_2\frac{\partial B_{20}}{\partial t_2}+e_2a_2B_{20}+e_2B_{20}=-e_1a_2B_{10} \tag{27}$$

Note that the definition

$$a_m\equiv\frac{b_m}{a},\qquad m=1,2, \tag{28}$$

has been used in Eq. 26 and Eq. 27 in order to simplify the notation.

The above system of partial differential equations can be solved exactly to obtain:

$$B_{10}=K_{B1}e^{-\frac{1}{2}[(a_1+1)e_1+(a_2+1)e_2-r]t_1}+K_{B2}e^{-\frac{1}{2}[(a_1+1)e_1+(a_2+1)e_2+r]t_2}, \tag{29}$$

$$B_{20} = -\frac{a}{2}\frac{(a_1+1)e_1-(a_2+1)e_2+r}{e_2 b_1}K_{B1}e^{-\frac{1}{2}[(a_1+1)e_1+(a_2+1)e_2-r]t_1} - \frac{a}{2}\frac{(a_1+1)e_1-(a_2+1)e_2-r}{2e_2 b_1}K_{B2}e^{-\frac{1}{2}[(a_1+1)e_1+(a_2+1)e_2+r]t_2}, \quad (30)$$

where

$$r \equiv \sqrt{e_1^2 - 2e_1e_2 - 2e_2a_2e_1 + 2e_1^2a_1 + e_2^2 + 2e_2^2a_2 - 2e_2e_1a_1 + e_2^2a_2^2 + 2e_2a_1e_1a_2 + e_1^2a_1^2}. \quad (31)$$

In the above expressions, the coefficients K_{B1} and K_{B2} are constants to be determined from the initial conditions for the distributions of neutrons and precursors.

It is important to note that Eq. 29 and Eq. 30 involve solely the slow time-scales, which means that this system of equations is no longer stiff. The development of the multiple-scales expansion can be stopped at this point, since the approximation obtained at this point is sufficient to obtain a first order solution. Collecting the results obtained yields the following first-order expressions for the concentrations of neutrons and precursors:

$$n = n_0 + e_1n_1 + e_2n_2 = D_0e^{a_1t_1+a_2t_2}e^{at_0} - e_1\frac{1}{a}B_{10} + e_2\frac{1}{a}B_{20} \quad (32)$$

$$c_1 = c_{10} = \frac{b_1}{a}D_0e^{a_1t_1+a_2t_2}e^{at_0} + B_{10} \quad (33)$$

$$c_2 = c_{20} = \frac{b_2}{a}D_0e^{a_1t_1+a_2t_2}e^{at_0} + B_{20} \quad (34)$$

Note that when the reactor is prompt critical (i.e., when $\rho = \beta$), then $a = 0$ while α_1 and α_2 become infinite, in which case the removable singularity in Eq. 32 through Eq. 34 causes numerical instabilities. This problem can be circumvented by replacing the exponential functions $e^{a_1t_1+a_2t_2}e^{at_0}$ with the exponential resulting from exact solution for one group of delayed neutrons, namely $e^{\frac{1}{2}(r-b-e-sq)t_0}$, which is equivalent to using first-order corrections to the zero-order result. This implies that the expression of the quantity a becomes

$$a = \frac{1}{2}\left(r - \sum_i b_i - e - q\right) \quad (35)$$

where

$$q \equiv \sqrt{a^2 + 2e\,a + e^2 + 4be}, \quad (36)$$

$$e \equiv \frac{\sum_i l_i b_i}{\sum_i b_i}\Lambda. \quad (37)$$

In Eq. 37, the summation runs over all the available groups of precursors. Furthermore, to avoid overestimating the production of precursors, the expression of the quantities α_m need to be redefined as

$$a_m \equiv \frac{b_m}{a+e_m}, \qquad m = 1, 2. \quad (38)$$

At this stage, the constants D_0, K_{B1}, and K_{B2}, which appear in Eq. 32 through Eq. 34 can be determined in terms of the initial conditions, n_0 and c_{0m}, for the initial conditiones, to obtain:

$$D_0 = \frac{1}{2}\frac{-a n_0 - e n_0 + q n_0 - 2\left(c_{01}e_1 + c_{02}e_2\right)}{q} \tag{39}$$

$$K_{B1} = \frac{-2a n_0 b_1 + 2D_0 a b_1 - 2e_1 K_{B2} b_1 + K_{B2} a e_1 (a_1 + 1) - K_{B2} a e_2 (a_2 + 1) - K_{B2} a r}{2e_1 b_1 - a e_1 (a_1 + 1) + a e_2 (a_2 + 1) - a r} \tag{40}$$

$$K_{B2} = \frac{\left(e_2 (a_2 + 1) - e_1 (a_1 + 1)\right) c_{01} - r c_{01} - 2c_{02}\frac{b_1}{a} e_2}{-2r} \tag{41}$$

.

The system of equations comprising Eq. 32 – Eq. 34, with the respective constants given by Eq. 35 through Eq. 41 will be called further on the "three-scale approximation". The initial distributions of neutrons and precursors can be defined either during the dynamic calculation (by the values at the end of the previous computational time-step) or from a standard steady state, e.g., $n_0 = 1$, $c_{0m} = \frac{b_m}{l_m \Lambda}$, $m = 1, 2$. The systems of equations which comprise the three-scale approximation for the P_1or P_3-equations is obtained by following an entirely similar path as for the point kinetics equations, above [16, 17, 18]. However, the corresponding mathematical derivations do not bring any new concepts, and are considerably more involved than those for the point kinetics equations; therefore, the derivations for the P_1-equations are relegated to the Appendix. The derivations for the P_3-equations can be found in the references.

3. ILLUSTRATIVE COMPUTATIONS USING THE THREE-SCALE APPROXIMATIONS

The illustrative computational results presented in this section aim at investigating the efficiency and accuracy of the three-scale approximation that was developed in the previous section.
It is of special interest to assess the accuracy of the three-scale approximation by comparison to the standard point kinetics equations with six groups of delayed neutrons. Of course, such a comparison must also take into account the fact that the standard six-group point kinetics equations need to be solved iteratively, so there will be a trade-off between solution accuracy and computational time requirements. The standard method for solving the point kinetics equations in accident analysis codes for fast reactors is an iterative numerical method based on the Kaganove algorithm [14]. Figure 1 illustrates the close agreement between the results produced by the iterative Kaganove algorithm for a fast reactor with 6 groups of delayed neutrons, undergoing a strong positive reactivity insertion (ρ = 0.9 \$), and the results obtained by using the three-scale approximation. For comparison, the results produced by the simpler two-scale approximation (corresponding with the reduction of the number of delayed neutron groups) which becomes increasingly worse in time are also depicted. The three-scale approximation produces very accurate results, practically indistinguishable from the Kaganove results.

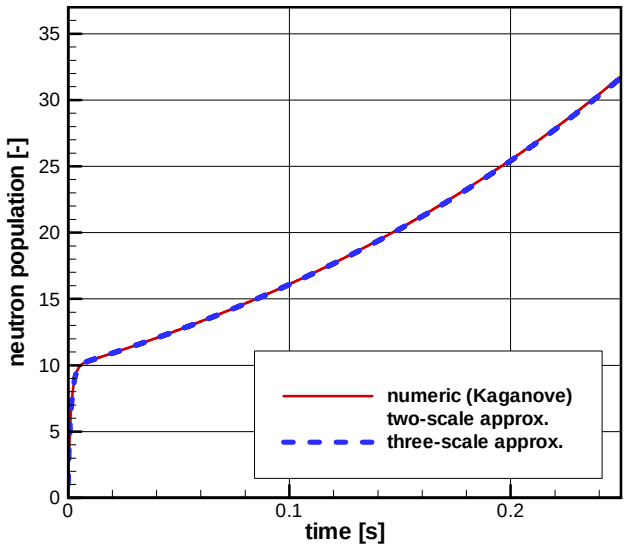

Figure 1: Neutron population following a positive reactivity insertion ($r = 0.9 \$$): comparison of two- and three-scale approx. with the iterative Kaganove algorithm

The time behavior of the difference between the standard iterative Kaganove algorithm with 6 groups of delayed neutrons and the three-scale approximation, depicted in Fig.2, indicates that the absolute value of this difference increases linearly in time, but remains quite small in absolute value. The relative difference stays below 0.1 ‰.

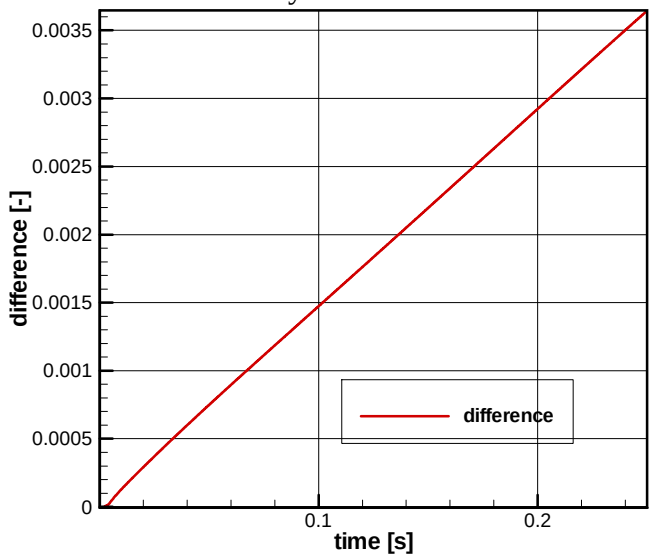

Figure 2: Evolution of the difference between the three-scale approximation solution and the iterative Kaganove algorithm (6 groups)

Having assessed the accuracy potential of the three-scale approximation, the remaining question to be addressed is that of evaluating the computational efficiency of this approximation. Since the respective approximation simply involves the computational evaluation of closed form expressions, its numerical efficiency if far superior to any method that would require the

numerical solution of the point kinetics equations. Thus, the distributions of prompt and delayed neutrons predicted by the three-scale approximation can be evaluated immediately, at any particular point in time, while the prediction of these distributions by using the Kaganove method necessarily requires an iterative process, by using time steps dictated either by the limitations of the neutron generation time and/or the convergence criterion selected by the user for the Kaganove algorithm. To illustrate the potential efficiency of the three-scale approximation, three cases have been investigated. The first case ("Case 0") involves a small stepwise reactivity perturbation (ρ =0.1 \$) that causes only a very small change in the neutron population. The second case ("Case 1") involves a large perturbation (ρ =0.9 \$), which causes a massive increase in the neutron population. The third case ("Case 2") involves a reactivity insertion in-between the first two cases (ρ =0.75 \$). Note that the iterative computations using the Kaganove algorithm (with 6 delayed groups) for "Case 0" and "Case 2" were stopped by the time limitation criterion (t_{max} = 0.1 s), while "Case 1" was stopped by the power limitation criterion (p_{max} = 5 times initial value).

The efficiency of the multi scale approximation solution is illustrated by computing the time reduction factor gained by using the three-scale approximation instead of the Kaganove algorithm, for the same level of accuracy. The results for this time reduction factor will henceforth be called, for short, "time gain", and are presented in Table 1 for the three cases described in the forgoing, as a function of the convergence criterion, ε, employed for the Kaganove algorithm. For the small perturbation (ρ = 0.1 \$) and the limiting time step of 0.1s, the time gain varies between (a factor of ca.) 2.6 and (a factor of ca.) 366. The time gain rises more dramatically for large perturbations (ρ = 0.9 \$), even when the reaching of the limiting factor in the neutron population causes a reduction of the overall time step to 0.001 s. The largest time gain is obtained for a relative big perturbation (ρ = 0.75 \$) in combination with a big over all time step, since, in this case, the limiting factors in time and neutron population are reached nearly simultaneously.

Table 1: Time gain for the three-scale approximation versus the iterative Kaganove algorithm (6 groups)

ε (Kaganove)	"Case 0" time gain	"Case 1" time gain	"Case 2" time gain
0.01	2.6	4.3	7.8
0.001	2.6	12.0	45.8
0.0001	24.6	49.1	368.4
0.00001	170.9	$>10^3$	$>10^4$
0.000005	365.9	$>10^4$	$>10^5$

As illustrated by the results shown in Table 1, above, the time gain for point kinetics calculations depends very strongly on the convergence criterion, ε; this strong dependence begs the question of the "best setting" of the value for ε to be used in the so-called "production" (as opposed to "research") codes, when dealing with changing reactivity values. For example, in computer codes, the convergence criterion, ε, is often set at a "default value", independent of the reactivity change; moreover, this "default value" can vary over a large range, depending on the specific code. Thus, in the SAS4A accident analysis code [11], which uses the point kinetics method, the default value for ε is set at $5*10^{-6}$. On the other hand, in the accident analysis code SIMMER-III [9], which uses the quasi-static method, the default value for ε is set at 0.001. The results shown in Table 1 indicate that the implementation of the three-scale approximation into (existent or future) production codes could avoid this problem.

Results from several illustrative computations for the space-time dependent problem using the three-scale approximation developed in the appendix will be presented following using an idealized case of a homogeneous slab, of infinite extent, subject to vanishing flux conditions, for both the prompt and delayed neutrons, on the extrapolated slab boundaries. The material properties characterizing the slab are as follows: $\left(v n \Sigma_f\right)^{-1} = 1.0\times10^{-06}$ s; $s_1 = 20$; $a_k = 0.2$; $b_1 = 4.277\times10^{-03}$; $b_2 = 3.223\times10^{-03}$; $\Lambda = 1.0\times10^{-06} s$; $l_1 = 2.926\text{s}^{-1}$; $l_2 = 0.02613\text{s}^{-1}$; $K_{x1} = K_{d1} = 0$; $K_{x2} = K_{d2} = 1$. The material properties (e.g., prompt and delayed neutron properties) chosen above are the same as for the point kinetics calculations, in order to facilitate the discussion of the multiple time-scale structure of the P_1- and P_3-equations by comparison to the point kinetics equations. The following additional quantities are used for the three-scale approximation to the P_3-equations: $s_2 = 100$, $s_3 = 120$, $K_{x3} = K_{x4} = K_{d3} = K_{d4} = 0$.
The illustrative computations to be presented next (in Figs. 3 through 9) are for a (moderate) reactivity insertion of ρ = 0.3 $. Recall also that the solution of the time-dependent diffusion equation for this simple paradigm geometry consists of the point-kinetics equations multiplied by a sine/cosine functional dependence in space. The actual forms taken on by the three-scale approximations of the prompt neutron fluxes for the diffusion, P_1, and P_3-equations are, respectively:

$$f_{dif}(x,t) = \left(-0.43e^{(-5252t)} - 1.44e^{(-0.607t)} + 2.86e^{(0.054t)}\right)\cos(3.4641x) \tag{45}$$

$$f_{P_1}(x,t) = \left(-0.11\times10^{-5}e^{(-2\times10^{7}t)} - 0.43e^{(-5305t)} - 1.44e^{(-0.607t)} + 2.86e^{(0.054t)}\right)\cos(3.4641x) \tag{46}$$

$$f_{P_3}(x,t) = \left(-0.11\times10^{-5}e^{(-1.2\times10^{8}t)} + 0.87\times10^{-9}e^{(-10^{8}t)} - 0.58\times10^{-9}e^{(-0.2\times10^{8}t)} - 0.43e^{(-5305t)} - 1.44e^{(-0.607t)} + 2.86e^{(0.054t)}\right)\cos(3.4668x)\Big) \tag{47}$$

Because of the symmetry inherent to the slab-geometry of the paradigm problem, the results to be presented in this Section are displayed only for (the negative) half of the x-axis. Figure 3 depicts the space-time distribution of the neutron flux, in the three-scale approximation, expressed by Eq. 46, for the P_1-equations.

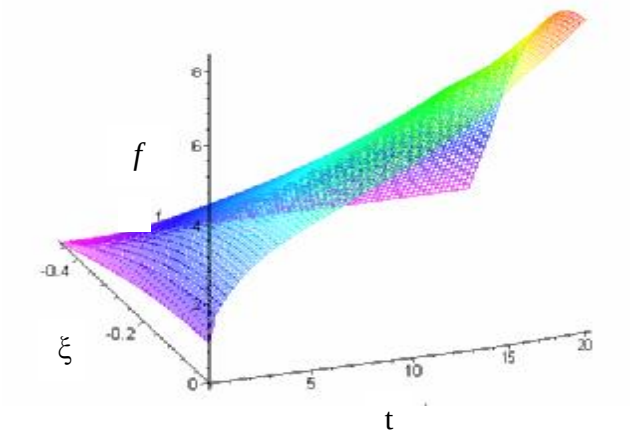

Figure 3: Neutron flux distribution, computed with the three-scale approximation of the P_1 equations, for a reactivity insertion of ρ=0.3$

As Fig. 3 clearly shows, only the three longest-lived terms influence the behavior of the prompt neutron flux on the time-scales relevant to nuclear reactors. The shorter lived terms [i.e., the first

term in Eq. 46, and the first three terms in Eq. 47] vanish far too quickly to visibly influence the rise of the prompt neutron flux on the reactor-type time scales considered in this work.

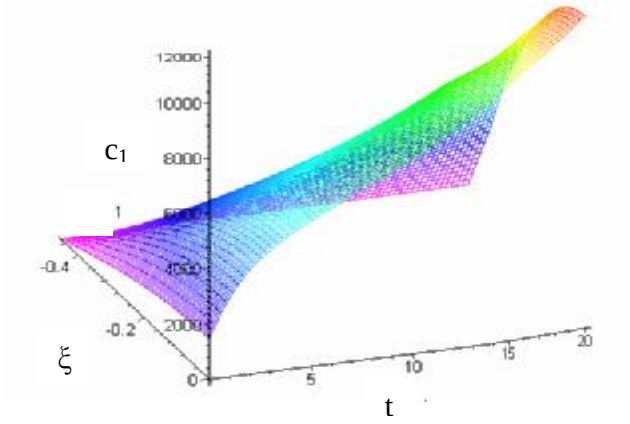

Figure 4: Distribution of delayed neutron prec. for the first group, computed with the three-scale approx. of the P_1 equations, for a reactivity insertion of r=0.3$.

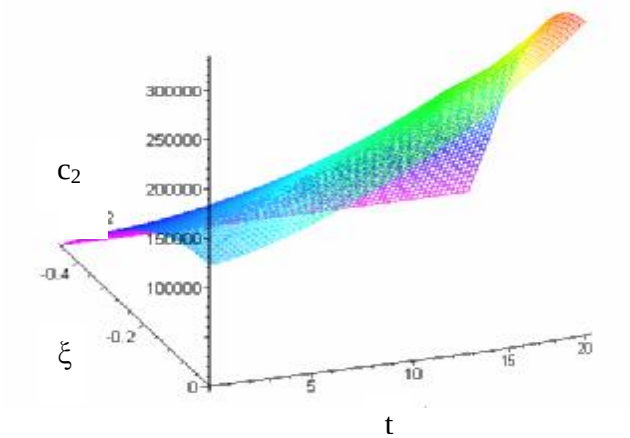

Figure 5: Distribution of delayed neutron prec. for the second group, computed with the three-scale approx. of the P_1 equations, for a reactivity insertion of r=0.3$.

Figures 4 and 5 depict, respectively, the space-time distributions of the first and the second groups of delayed neutrons in the three-scale approximations. The cosine-distribution of both the prompt and delayed neutrons, in the spatial direction is also apparent in Figs 3 to 5, as expected in view of the homogeneous infinite slab geometry considered in these illustrative examples. The neutron fluxes given by Eq. 45 and 47, which express the three-scale approximations corresponding to the diffusion and P_3-equations, respectively, show a similar space-time behavior as that depicted in Figure 3. The differences between the fluxes computed using Eqs. 45, 46, and 47, starting all computations from identical initial conditions and effecting the same reactivity insertion of ρ=0.3$, are depicted in Figs. 6 and 7. Both of these figures display a positive peak in the time interval below 0.001 s, after which the differences vanish rapidly in time. The reasons for the shape of this peak become apparent by examining Eqs. 46 and 47. The three-scale approximations for the P_1 and for the P_3-equations contain one and, respectively, three additional exponential functions, with large negative exponents; furthermore, the respective terms (which

simulate the prompt neutron production) are not identical. The additional exponential terms appear because of the time-derivatives of the higher-order spherical harmonics neutron fluxes. These derivative terms are discarded when deriving the diffusion approximation from the neutron transport equation. However, if the space and time coordinates are separated ab initio (as practiced within the improved quasi-static method [22]), these additional exponential functions would not appear either within the corresponding diffusion or the P_1 or P_3-equations. In other words, imposing an ab initio separation of space and time for solving the neutron transport equation would cause the time behavior of the P_1 and/or P_3 approximations to be the same as that of the diffusion approximation; the differences shown in Eqs. 45, 46, and 47 for the respective three-scale expressions for the neutron flux arise from the fact that the starting equations the respective P_1 - and P_3- approximations were obtained without having imposing a space-time separation on the full-fledged neutron transport equation. To summarize, the differences in the respective prompt terms and the terms which appear additionally in Eqs. 46 and 47 (but do not appear in the diffusion approximation described by Eq. 45) represent the transport effects on the time-behavior of the neutron distribution within the paradigm slab reactor.

The absolute value of the peak depicted in Figs. 6 and 7 depends on a_k and other system parameters; the peak maximum is attained in the beginning of the transient, and is about 1% of the absolute change in the neutron flux for this special case (ρ=0.3$). Afterwards, the exponentials with the largest negative exponents decay very rapidly. For longer time values, the differences depicted in Figs. 7 and 8 vanish, since the long-term behavior of Eqs. 45, 46 and 47 is governed by identical terms.

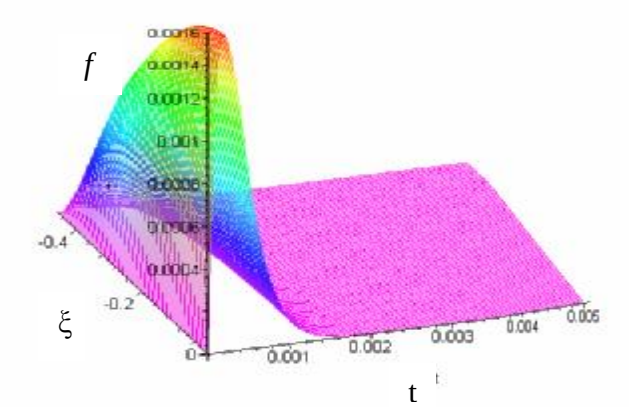

Figure 6: Difference [$f_{P_1}(t) - f_{dif}(t)$], using Eqs. (85) and (84).

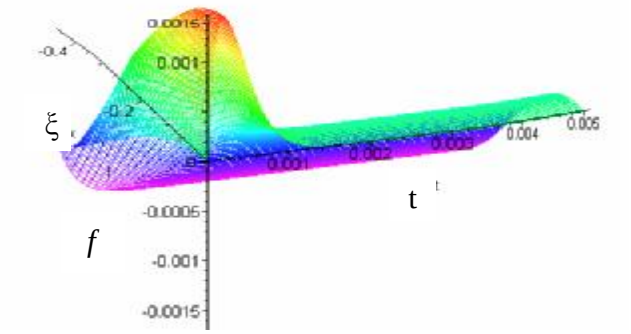

Figure 7: Difference [$f_{P_3}(t) - f_{dif}(t)$], using Eqs. (86) and (84)

Comparing Figures 6 and 7 indicates that the absolute value and the time duration of the peak for the three-scale approximation of the P_3-equations are close to the results obtained using the three-scale approximation of the P_1-equations. The time-dependent differences, which are due to the additional two exponential functions in $f_{P_3}(t)$, are relevant only on a time scale which is shorter than the time scale considered for calculations in nuclear reactors. On the other hand, the spatial-dependent differences arise from the slightly different arguments of the cosine functions that appear in Eqs. 47 and 45, respectively. The foregoing observations indicate that the considerable additional work involved in using the three-scale approximation for the P_3-equations [17, 18] brings little improvement of the quality of the results, as far as their time-behavior is concerned, as compared to using the three-scale approximation for the P_1-equation instead of the three-scale approximation for the diffusion equation. Hence, the three-scale approximation for the P_3-equation may be advantageous to use for a more accurate modeling of the spatial distribution of the neutron flux (especially if the additional terms with the constants K_3 and K_4 are needed), but the three-scale approximation for the P_1-equation would suffice for modeling most transients of interest for nuclear reactors.

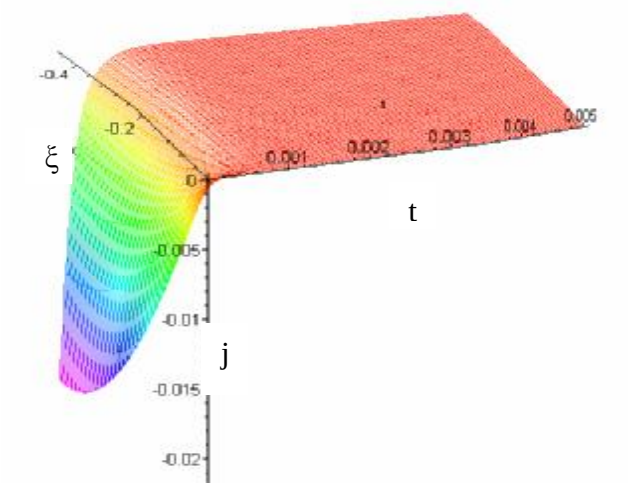

Figure 8: Difference [$j_{P_1}(t) - j_{dif}(t)$], computed with the three scale approximation for the P_1 and the diffusion approximation, respectively.

Figure 8 depicts the distribution, in space and time, of the difference [$j_{P_1}(t) - j_{dif}(t)$], computed by using the three scale approximations for the P_1- and the diffusion equations, respectively. The difference between these two approximations is significant, reaching a peak of ca. 20%, for a very short time interval, immediately after initiating the transient computations. The explanation of this difference is provided by examining the respective equations: on the one hand, the three-scale approximation for the neutron current computed from the diffusion equation, $j_{dif}(t)$, is obtained by a multiplying the standard point kinetics solution by the respective stationary spatial distribution; on the other hand, all of the short-time dependent terms drop out during the development of $j_{P_1}(t)$, as indicated by Eq. A.72. The corresponding result for the three-scale approximation of the neutron current corresponding to the P_3-equations of the same structure, and its behavior in space-time is very similar to that of $j_{P_1}(t)$.

The behavior in time of the (space-time dependent) precursor distributions is nearly identical for the three-scale approximations of the diffusion, the P_1-, and the P_3-equations, since the dominating exponential functions are identical in the respective approximations. The differentiated effects of the reactivity insertion's magnitude on the three-scale approximations for the diffusion and the P_1-equations, respectively, are illustrated in Fig. 9, for a prompt critical reactivity insertion. This large reactivity insertion highlights not only the short-time behavior of the difference $[f_{P_1}(t) - f_{dif}(t)]$, but also underscores the fact that, for large perturbations, this difference does not vanish as time progresses, as was the case for the smaller reactivity insertion (of ρ=0.3$) considered in Fig. 6. As shown in Fig. 9, the difference $[f_{P_1}(t) - f_{dif}(t)]$ increases over the time interval considered in the computation, with the rate of increase commencing at about 1.8 % and reaching an asymptotic value of about 1.3 % of the absolute change in neutron flux, during the transient computation for this paradigm homogeneous slab reactor. The time behavior of the difference $[f_{P_1}(t) - f_{dif}(t)]$ confirms the expectation that the influence of the three-scale approximation for the P_1-equations is more pronounced for strong transients, in which the prompt neutron production dominates the overall time evolution of the neutron distribution. The differences in the corresponding three-scale approximations for the precursor concentrations are not sensitive to the magnitude of reactivity insertion, for reasons already discussed in relation to Figs. 5 and 6.

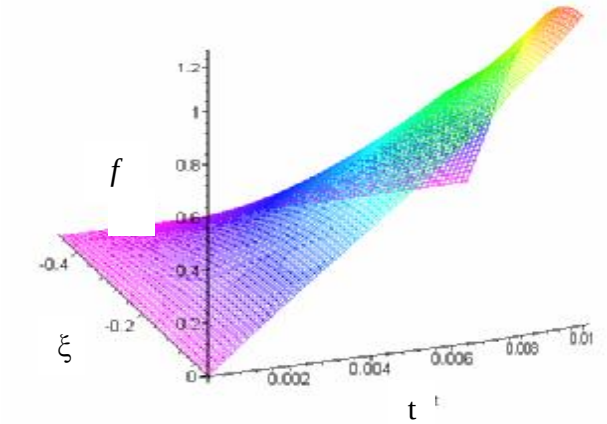

Figure 10: Difference $[f_{P_1}(t) - f_{dif}(t)]$ for a prompt critical reactivity insertion.

3. CONCLUSIONS

The method of multiple scale expansion offers a new way for the development of very accurate and effective multi scale approximation functions for different approximations of the time dependent Boltzmann equation with delayed neutrons. The developed multi scale analytic approximation functions are powerful and effective tools for the analysis of the time behavior of multiplying systems with delayed neutron production.

The analysis of the accuracy of the multi scale approximation solution has shown very good agreement in the comparison with the standard iterative solution with 6 groups of delayed neutrons on the basis of the Kaganove algorithm. Although a time gain is achieved for every configuration, the actual amount of the time gain depends strongly on the system parameters and the convergence criterion of the numerical algorithm. The gain varies between factors of 3 up to 10^5 for the test calculations.

It is also important to note that, although the three-scale approximation of this work is limited to two groups of delayed neutrons; this limitation could be readily removed without loss of consistency if the number time scales were to be increased to four or five scales. In such a case, the multi-scale approximation would be developed by using the same already described strategy as illustrated in Section II and also in the appendix; for five time scales, for example, the corresponding versions of Eq. 26 and Eq. 27 would constitute a system of fourth order instead of the system of the second order.

The multiple scale expansion method has been used to develop closed-form three-scale approximations for the time dependent P_1-equations for a homogeneous multiplying material, in planar geometry, with two groups of delayed neutrons. Closed-form three-scale approximations have been obtained for the neutron flux and its higher-order spherical harmonics, as well as for the precursors for two groups of delayed neutrons. The development of these three-scale approximations did not rely on imposing separation of space and time; furthermore, they offer the possibility of a direct investigation of the differences between the P_1-, P_3-, and diffusion equations, respectively. Thus, significant differences are observed regarding the time-behavior of the various approximations for the neutron current, smaller differences are observed regarding the differences in the time-behavior of the various expressions for the neutron flux, while the distinctions between the various approximations for the precursor distributions are negligible. Furthermore, the three-scale approximations for the P_1- and P_3-equations have been shown to be superior to the results offered by the improved quasistatic methods described in the literature, particularly for the shortest time scales, in the presence of large reactivity insertions.

One way for implementing multiple time-scale approximations for creating new and efficient solutions strategies for the time-dependent neutron transport equations with delayed neutrons is by splitting the main matrix of a neutron transport code by using the closed-form expressions, developed in this work, for the three-scale approximation to the P_1-equations.

Such a splitting of the main matrix of a neutron transport code would lead to several sub-matrices, each of them corresponding to the respective time scales underlying the multiple scale expansion. These single sub-matrices would be considerably smaller than the main matrix, and could therefore be inverted directly, because these sub-matrices would no longer be stiff. In principle, such a procedure would amount to an inversion of the main matrix by block partitioning (each block corresponding to a specific time-scale); such an inversion procedure is usually more efficient than the standard iterative one. Thus, the gain in efficiency offered by implementing closed-forms expressions derived from multiple-time expansions is not obtained from potential use of the larger possible time steps due to the analytical approximation solution but from the more efficient mathematical methods. Furthermore, closed-forms expressions derived from multiple-time expansions can also be used in concert with customary acceleration methods.

To summarize, the method of multiple scale expansion offers a new way for developing very accurate and effective approximations for solving typical stiff-systems, such as the time-dependent neutron transport and/or diffusion equations with delayed neutrons. Further extensions, beyond the paradigm examples provided in this work, would be the consideration of more than three time-scales and a combined expansion that would separate multiple-scales not only in time but also in space.

REFERENCES

1. K. O. Ott, R. J. Neuhold: *Introductory Nuclear Reactor Dynamics*, American Nuclear Society, La Grange Park Il (1985).
2. J. Barclay Andrews II, K. F. Hansen: „Numerical Solution of the Time-Dependent Multigroup Diffusion Equations", *Nuclear Science and Engineering*, **Vol. 31**, pp. 304-313 (1968).
3. J. B. Yasinsky: „The Solution of the Space-Time Neutron Group Diffusion Equations by a Time-Discontinuous Synthesis Method", *Nuclear Science and Engineering*, **Vol. 29**, pp. 381 (1967).
4. K. Ott, J. Madell: „Quasistatic Treatment of Spatial Phenomena in Reactor Dynamics", *Nuclear Science and Engineering*, **Vol. 26**, pp. 563-565 (1966).
5. G. R. Keepin: *Physics of Nuclear Kinetics*, Addison Wesley, Reading (1965).
6. S. Langenbuch, W. Maurer, W. Werner: "Coarse-Mesh Flux-Expansion Method for the Analysis of Space-Time Effects in Large Light Water Reactor Cores", *Nuclear Science and Engineering*, **Vol. 63**, pp. 437-456 (1977).
7. J. J. Dorning: "Modern Coarse Mesh Methods – A New Development of the '70's", *Topl. Mtg. Computational Methods in Nucl. Eng.*, Williamsburg VA (1979). Vol. 3-1
8. K. S. Smith: *An Analytic Nodal Method for Solving the Two-Group, Multidimensional, Static and Transient Neutron Diffusion Equations*, Dissertation at Massachusetts Institute of Technology (1979).
9. S. Kondo et al.: "SIMMER-III: An Advanced Computer Program for LMFBR Severe Accident Analysis", *ANP'92*, Tokyo, Japan (1992).
10. H. U. Wider et al.: *Comparative Analysis of a Hypothetical Loss-of-Flow Accident in an Irradiated LMFBR Core Using Different Computer Models for a Common Benchmark Problem*, EUR 11925 EN (1989).
11. *The SAS4A LMFBR Accident Analysis Code System*, ANL/RAS 83-38 revision 2 (1988).
12. J. Kevorkian, J. D. Cole: *Multiple Scale and Singular Perturbation Methods*, Applied Mathematical Science, **Vol. 114**, Springer, New York (1996).
13. G. Sandri: "A New Method of Expansion in Mathematical Physics", *Il Nuovo Cimento*, **Vol. 36**, pp. 67-93 (1965).
14. J. J. Kaganove: *Numerical Solution of the One-Group Space-Independent Reactor Kinetics Equations for Neutron Density Given the Excess Reactivity*, Argonne National Lab. ANL-6132 (1960).
15. SIMMER-III: *A Computer Program for LMFR Core Disruptive Accident Analysis (Version 2.G)*, JNC TN 9400 2001-002 (2000).
16. B. R. Merk and D. G. Cacuci: "Multiple Time-Scales Expansions for Neutron Kinetics: II. Illustrative Application to P1 and P3 Equations", accepted by *Nuclear Science and Engineering* (2005).
17. B. R. Merk and D. G. Cacuci: "Multiple Time-Scales Expansions for Neutron Kinetics: I. Illustrative Application to the Point Kinetics Model", accepted by *Nuclear Science and Engineering* (2005).
18. B. R. Merk: *Eine mehrskalige Näherungslösung für die zeitabhängige Boltzmann-Transportgleichung*, FZKA 6963, Karlsruhe (2003)
19. J. Duderstadt, L. Hamilton: *Nuclear Reactor Analysis*, John Wiley & Sons, Inc., New York (1976).

20. J. J. Duderstadt, W. R. Martin: *Transport Theory*, John Wiley & Sons, New York (1979).
21. M. Clark Jr., K. F. Hansen: *Numerical Methods of Reactor Analysis*, Nuclear Science and Technology 3, Academic Press, New York (1964)
22. S. Goluoglu, H. L. Dodds: "A Time-Dependent, Three-Dimensional Neutron Transport Methodology", *Nuclear Science and Engineering*, **Vol. 139**, pp. 248-261 (2001)

APPENDIX A

Three-Scale Expansion Approximations for the P_1-Equations

Using standard notation, the time-dependent P_1-approximation to the neutron transport equations with n groups of delayed neutrons, in a one-dimensional homogeneous slab geometry, comprises the following coupled partial differential equations:

$$\frac{1}{\mathrm{v}}\frac{\partial f(x,t)}{\partial t}+\frac{\partial j(x,t)}{\partial x}+\Sigma_a f(x,t)=(1-b)n\Sigma_f f(x,t)+\sum_{i=1}^{n} l_i C_i(x,t), \tag{A.1}$$

$$\frac{1}{\mathrm{v}}\frac{\partial j(x,t)}{\partial t}+\frac{1}{3}\frac{\partial f(x,t)}{\partial x}+\Sigma_{tr} j(x,t)=0, \tag{A.2}$$

$$\frac{\partial C_i(x,t)}{\partial t}=b_i n\Sigma_f f(x,t)-l_i C_i(x,t), \qquad i=1,\ldots,n. \tag{A.3}$$

Prior to applying multiple-scale expansion method, the above equations need to be transformed in dimensionless form by defining the following quantities:

$$t \equiv \mathrm{v}(n\Sigma_f)t, \tag{A.4}$$

$$x \equiv (n\Sigma_f)x, \tag{A.5}$$

$$c(t)\equiv \mathrm{v}\,C(t), \tag{A.6}$$

$$s_1 \equiv \frac{\Sigma_{tr}}{n\Sigma_f}, \tag{A.7}$$

$$a_0 \equiv \frac{n\Sigma_f-\Sigma_a}{n\Sigma_f} \equiv a_k + a, \tag{A.8}$$

where the static criticality value of the infinite system, denoted by a_k , is defined as

$$a_k \equiv \frac{n\Sigma_f-\Sigma_a}{n\Sigma_f}, \tag{A.9}$$

while the transient reactivity change in the system, denoted by a , is defined as

$$a \equiv \frac{\Sigma_{at}-n\Sigma_{ft}}{n\Sigma_f}+b \tag{A.10}$$

.

Using the above definitions in Eqs. A.1 – A.3, and limiting the resulting equations to two groups of delayed neutrons yields the following form for the non-dimensional P1-equations:

$$\frac{\partial f}{\partial t}+\frac{\partial j}{\partial x}-(a_k+a)f=e_1 c_1+e_2 c_2, \tag{A.11}$$

$$\frac{\partial j}{\partial t}+\frac{1}{3}\frac{\partial f}{\partial x}+s_1 j=0, \tag{A.12}$$

$$\frac{\partial c_m}{\partial t} = b_m f - e_m c_m, \qquad m = 1,2. \tag{A.13}$$

As in Section II, we introduce into Eqs. A.11– A.13 the dimensionless time parameters

$$t_0 = t, \quad t_1 = e_1 t, \quad t_2 = e_2 t, \tag{A.14}$$

and expand the time derivative operator in the series

$$\frac{d}{dt} = \frac{\partial}{\partial t_0} + e_1 \frac{\partial}{\partial t_1} + e_2 \frac{\partial}{\partial t_2} + \mathbf{K} \tag{A.15}$$

It follows that the neutron flux f, the neutron current j and the precursor concentrations c_m can be represented in infinite series of the form

$$f = f_0 + e_1 f_1 + e_2 f_2 + \mathbf{K} \tag{A.16}$$

$$j = j_0 + e_1 j_1 + e_2 j_2 + \mathbf{K} \tag{A.17}$$

$$c_m = c_{m0} + e_1 c_{m1} + e_2 c_{m2} + \mathbf{K} \qquad m = 1,2. \tag{A.18}$$

Introducing Eqs. A.14 – A.18 into Eqs. A.11 – A.13 and equating the coefficients of like powers of e_1 and, respectively, e_2, will yield a series of systems of equations for the respective functions in Eqs. A.16 – A.18. Thus, the zero-order terms (which are independent of e_1 and e_2, of course) yield the following equations for the neutron flux, f_0, the neutron current, j_0, and the precursor concentrations, c_{m0}:

$$\frac{\partial f_0}{\partial t_0} + \frac{\partial j_0}{\partial x} - (a_k + a) f_0 = 0, \tag{A.19}$$

$$\frac{\partial j_0}{\partial t_0} + \frac{1}{3}\frac{\partial f_0}{\partial x} + s_1 j_0 = 0, \tag{A.20}$$

$$\frac{\partial c_{m0}}{\partial t_0} = b_m f_0, \qquad m = 1,2. \tag{A.21}$$

Equations A.19 – A.21 describe the behavior of neutron population on the time scale of prompt neutron production. Their solution can be obtained analytically, and will be shown to contain an exponential function in time accompanied by either a linear combination of two exponential functions in space, if the static reactivity is negative (i.e., if $a_k < 0$), or by a linear combination of trigonometric functions in space, if the static reactivity is negative (i.e., if $a_k > 0$).

The case of negative static reactivity ($a_k < 0$)

In this case, the fundamental solution of Eqs. A.19 – A.21 can be written in the following form:

$$f_0 = \left(K_{x1} e^{e_a x} + K_{x2} e^{-e_a x}\right) A_{0n} e^{e_{en} t_0}, \quad n = 1,2; \tag{A.22}$$

$$j_0 = \left(K_{x1} e^{e_a x} - K_{x2} e^{-e_a x}\right) j_{en} A_{0n} e^{e_{en} t_0} + C_{0n} e^{-s_1 t_0}, \quad n = 1,2; \tag{A.23}$$

$$c_{10} = \left(K_{x1} e^{e_a x} + K_{x2} e^{-e_a x}\right) \frac{b_1}{e_{en}} A_{0n} e^{e_{en} t_0} + B_{10}(x), \quad n = 1,2; \tag{A.24}$$

$$c_{20} = \left(K_{x1} e^{e_a x} + K_{x2} e^{-e_a x}\right) \frac{b_2}{e_{en}} A_{0n} e^{e_{en} t_0} + B_{20}(x), \quad n = 1,2. \tag{A.25}$$

The following notations have been used in Eqs. A.22– A.25:

$$e_a \equiv \sqrt{-3 a_k s_1}, \tag{A.26}$$

$$B_{10}(x) \equiv b_{01}\left(K_{d1}e^{e_a x} + K_{d2}e^{-e_a x}\right), \tag{A.27}$$

$$B_{20}(x) \equiv b_{02}\left(K_{d1}e^{e_a x} + K_{d2}e^{-e_a x}\right), \tag{A.28}$$

$$e_{en} \equiv -Z_n e_a + a_k + a, \quad n = 1,2; \tag{A.29}$$

$$j_{en} \equiv Z_n, \quad n = 1,2. \tag{A.30}$$

The variables Zn ($n = 1,2$), which appear above in the expressions of e_{en} and j_{en}, denote the two roots of the quadratic equation

$$3Z^2 e_a + \left(-3a_k - 3s_1 - 3a\right) Z - e_a = 0. \tag{A.31}$$

The quantities A_{0n} and C_{0n}, which appear in Eqs. A.22 – A.25, are independent of τ_0, but may be functions of τ_1 and τ_2. Therefore, these quantities must be determined by using the first order equations in e_1 and e_2, which read

$$e_1\frac{\partial f_1}{\partial t_0} + e_2\frac{\partial f_2}{\partial t_0} + e_1\frac{\partial f_0}{\partial t_1} + e_2\frac{\partial f_0}{\partial t_2} + e_1\frac{\partial j_1}{\partial x} + e_2\frac{\partial j_2}{\partial x} - e_1(a_k + a)f_1 - e_2(a_k + a)f_2 = e_1 c_{10} + e_2 c_{20}, \tag{A.32}$$

$$e_1\frac{\partial j_1}{\partial t_0} + e_2\frac{\partial j_2}{\partial t_0} + e_1\frac{\partial j_0}{\partial t_1} + e_2\frac{\partial j_0}{\partial t_2} + e_1\frac{1}{3}\frac{\partial f_1}{\partial x} + e_2\frac{1}{3}\frac{\partial f_2}{\partial x} + e_1 s_1 j_1 + e_2 s_1 j_2 = 0, \tag{A.33}$$

$$e_1\frac{\partial c_{m1}}{\partial t_0} + e_2\frac{\partial c_{m2}}{\partial t_0} + e_1\frac{\partial c_{m0}}{\partial t_1} + e_1\frac{\partial c_{m0}}{\partial t_2} = e_1 b_m f_1 + e_2 b_m f_2 - e_m c_{m0}, \qquad m = 1,2. \tag{A.34}$$

Next, the quantities c_{10} and c_{20} are eliminated from appearing in Eqs. A.31 – A.34 by using Eqs. A.24 and A.25 together with the differentiated forms of Eqs. A.22 and A.23, thus obtaining a system of four equations for the quantities f_1, f_2, j_1, and j_2 (which represent the neutron flux and current in the time scales of the delayed neutrons). The resulting equations are then required to be independent of τ_0 (which corresponds to the zeroth-order terms in ε); this requirement yields the following equations for determining A_{0n} and C_{0n}:

$$e_1\left(\frac{\partial A_{0n}}{\partial t_1} - \frac{b_1}{e_{en}}A_{0n}\right) + e_2\left(\frac{\partial A_{0n}}{\partial t_2} - \frac{b_2}{e_{en}}A_{0n}\right) = 0, \quad n = 1,2; \tag{A.35}$$

$$e_1\left(K_{x1}e^{e_a x} - K_{x2}e^{-e_a x}\right) j_{en}\frac{\partial A_{0n}}{\partial t_1}e^{e_{en}t_0} + e_1\frac{\partial C_{0n}}{\partial t_1}e^{-s_1 t_0} + e_2\left(K_{x1}e^{e_a x} - K_{x2}e^{-e_a x}\right) j_{en}\frac{\partial A_{0n}}{\partial t_2}e^{e_{en}t_0} + e_2\frac{\partial C_{0n}}{\partial t_2}e^{-s_1 t_0} = 0, \quad n = 1,2. \tag{A.36}$$

Solving the above equations gives the following expressions for A_{0n} and C_{0n} as functions of the slower time-scales τ_1 and τ_2

$$A_{0n}(t_1, t_2) = D_{0n}e^{\frac{b_1}{e_{en}}t_1 + \frac{b_2}{e_{en}}t_2}, \quad n = 1,2; \tag{A.37}$$

$$C_{0n}(t_1, t_2) = -j_{en}D_{0n}e^{\frac{b_1}{e_{en}}t_1 + \frac{b_2}{e_{en}}t_2}e^{e_{en}+s_1 t_0}\left(K_{x1}e^{e_a x} - K_{x2}e^{-e_a x}\right) + C_{1n}, \quad n = 1,2. \tag{A.38}$$

As indicated by the above expressions, the functions A_{0n} and C_{0n} introduce the influence of the delayed neutron production into Eqs. A.22– A.25, which describe the short time scales associated with the production of prompt neutrons. Equations A.37 and A.38 are now used to simplify Eqs.

A.32 – A.34, which makes it possible to solve the latter analytically to obtain the following expressions for the neutron fluxes f_1 and f_2, and the neutron currents j_1 and j_2:

$$f_1 = \left(K_{x1}e^{e_a x} + K_{x2}e^{-e_a x}\right)A_{1n}e^{e_{en}t_0} + z_{1e}b_{01}\left(K_{d1}e^{e_a x} + K_{d2}e^{-e_a x}\right) \qquad n=1..2 \tag{A.39}$$

$$f_2 = \left(K_{x1}e^{e_a x} + K_{x2}e^{-e_a x}\right)A_{2n}e^{e_{en}t_0} + z_{1e}b_{02}\left(K_{d1}e^{e_a x} + K_{d2}e^{-e_a x}\right) \qquad n=1..2 \tag{A.40}$$

$$j_1 = \left(K_{x1}e^{e_a x} - K_{x2}e^{-e_a x}\right)j_{en}A_{1n}e^{e_{en}t_0} + z_{2e}b_{01}\left(K_{d1}e^{e_a x} - K_{d2}e^{-e_a x}\right) \qquad n=1..2 \tag{A.41}$$

$$j_2 = \left(K_{x1}e^{e_a x} - K_{x2}e^{-e_a x}\right)j_{en}A_{2n}e^{e_{en}t_0} + z_{2e}b_{02}\left(K_{d1}e^{e_a x} - K_{d2}e^{-e_a x}\right) \qquad n=1..2 \tag{A.42}$$

The following definitions have been used in the above expressions:

$$z_{1e} \equiv -\frac{1}{a}, \tag{A.43}$$

$$z_{2e} \equiv \frac{1}{3as_1}e_a. \tag{A.44}$$

The quantities b_{01} and b_{02} in Eqs. A.39 – A.42 must be independent of the fast time scale τ_0, but may depend on the slower time scales τ_1 and τ_2. The later dependence is determined by following the same procedures as for the quantities A_{0n} and C_{0n}; this procedure ultimately leads to the conditions

$$e_1\frac{\partial b_{01}}{\partial t_1} + e_2\frac{\partial b_{01}}{\partial t_2} + e_1a_1b_{01} + e_1b_{01} = -e_2a_1b_{02}, \tag{A.45}$$

$$e_1\frac{\partial b_{02}}{\partial t_1} + e_2\frac{\partial b_{02}}{\partial t_2} + e_2a_2b_{02} + e_2b_{02} = -e_1a_2b_{01}, \tag{A.46}$$

where

$$a_m \equiv -b_m z_{1e}, \quad m=1,2. \tag{A.47}$$

The closed-form solution of Eqs. A.45 and A.46 can be written in the form

$$b_{01} = K_{B1}e^{-\frac{1}{2}[(a_1+1)e_1+(a_2+1)e_2-sr]t} + K_{B2}e^{-\frac{1}{2}[(a_1+1)e_1+(a_2+1)e_2+sr]t}, \tag{A.48}$$

$$\begin{aligned} b_{02} = &-\frac{a}{2}\frac{(a_1+1)e_1-(a_2+1)e_2+sr}{e_2b_1}K_{B1}e^{-\frac{1}{2}[(a_1+1)e_1+(a_2+1)e_2-sr]t} \\ &-\frac{a}{2}\frac{(a_1+1)e_1-(a_2+1)e_2-sr}{2e_2b_1}K_{B2}e^{-\frac{1}{2}[(a_1+1)e_1+(a_2+1)e_2+sr]t}, \end{aligned} \tag{A.49}$$

where

$$sr \equiv \sqrt{e_1^2 - 2e_1e_2 - 2e_2a_2e_1 + 2e_1^2a_1 + e_2^2 + 2e_2^2a_2 - 2e_2e_1a_1 + e_2^2a_2^2 + 2e_2a_1e_1a_2 + e_1^2a_1^2}. \tag{A.50}$$

After redefining various constants, the results obtained thus far can be collected to obtain the following three-scale, two-group approximation to the time-dependent P_1-equations:

$$\begin{aligned} f = f_0 + e_1f_1 + e_2f_2 = &\left(K_{x1}e^{e_a x} + K_{x2}e^{-e_a x}\right)\sum_n D_{0n}e^{\frac{b_1}{e_{en}}t_1 + \frac{b_2}{e_{en}}t_2}e^{e_{en}t_0} \\ &+ e_1z_{1e}\left(K_{d1}e^{e_a x} + K_{d2}e^{-e_a x}\right)b_{01} + e_2z_{1e}\left(K_{d1}e^{e_a x} + K_{d2}e^{-e_a x}\right)b_{02}, \quad n=1,2; \end{aligned} \tag{A.51}$$

$$\begin{aligned} j = j_0 + e_1j_1 + e_2j_2 = \\ e_1z_{2e}\left(K_{d1}e^{e_a x} - K_{d2}e^{-e_a x}\right)b_{01} + e_2z_{2e}\left(K_{d1}e^{e_a x} - K_{d2}e^{-e_a x}\right)b_{02}, \end{aligned} \tag{A.52}$$

$$c_1 = c_{10} = \left(K_{x1}e^{e_a x} + K_{x2}e^{-e_a x}\right)\sum_n \frac{b_1}{e_{en}} D_{0n} e^{\frac{b_1}{e_{en}}t_1 + \frac{b_2}{e_{en}}t_2} e^{e_{en}t_0} + \left(K_{d1}e^{e_a x} + K_{d2}e^{-e_a x}\right)b_{01}, \quad n = 1,2; \quad \text{(A.53)}$$

$$c_2 = c_{20} = \left(K_{x1}e^{e_a x} + K_{x2}e^{-e_a x}\right)\sum_n \frac{b_2}{e_{en}} D_{0n} e^{\frac{b_1}{e_{en}}t_1 + \frac{b_2}{e_{en}}t_2} e^{e_{en}t_0} + \left(K_{d1}e^{e_a x} + K_{d2}e^{-e_a x}\right)b_{02}, \quad n = 1,2. \quad \text{(A.54)}$$

The case of positive static reactivity ($a_k > 0$)

In this case, the solution of Eqs. A.19– A.21can be written in the following form:

$$f_0 = \left[K_{x1}\sin(x_t x) + K_{x2}\cos(x_t x)\right] A_{0n} e^{e_{tn}t_0}, \qquad n = 1,2; \quad \text{(A.55)}$$

$$j_0 = \left[-K_{x1}\cos(x_t x) + K_{x2}\sin(x_t x)\right] j_{tn} A_{0n} e^{e_{tn}t_0} + C_{0n}e^{-s_1 t_0}, \qquad n = 1,2; \quad \text{(A.56)}$$

$$c_{10} = \left[K_{x1}\sin(x_t x) + K_{x2}\cos(x_t x)\right]\frac{b_1}{e_{tn}} A_{0n} e^{e_{tn}t_0} + B_{10}(x), \qquad n = 1,2; \quad \text{(A.57)}$$

$$c_{20} = \left[K_{x1}\sin(x_t x) + K_{x2}\cos(x_t x)\right]\frac{b_2}{e_{tn}} A_{0n} e^{e_{tn}t_0} + B_{20}(x), \qquad n = 1,2. \quad \text{(A.58)}$$

The following definitions were used in the above expressions:

$$x_t \equiv \sqrt{3a_k s_1}, \quad \text{(A.59)}$$

$$j_{en} \equiv Z_n, \qquad n = 1,2; \quad \text{(A.60)}$$

$$e_{tn} \equiv -Z_n x_t + a_k + a, \quad n = 1,2; \quad \text{(A.61)}$$

$$B_{10}(x) = b_{01}\left[K_{d1}\sin(x_t x) + K_{d2}\cos(x_t x)\right], \quad \text{(A.62)}$$

$$B_{20}(x) = b_{02}\left[K_{d1}\sin(x_t x) + K_{d2}\cos(x_t x)\right]. \quad \text{(A.63)}$$

In Eqs. A.60 and A.61, the quantities $Z_n, (n = 1,2),$ denote the two roots of the quadratic equation:

$$3Z^2 x_t + \left(-3a_k - 3s_1 - 3a\right)Z + x_t = 0. \quad \text{(A.64)}$$

Furthermore, the first-order neutron fluxes f_1 and f_2, and neutron currents j_1 and j_2 take on the forms

$$f_1 = \left[K_{x1}\sin(x_t x) + K_{x2}\cos(x_t x)\right] A_{1n} e^{e_{tn}t_0} + z_{1t} b_{01}\left[K_{d1}\sin(x_t x) + K_{d2}\cos(x_t x)\right], \; n = 1,2; \quad \text{(A.65)}$$

$$f_2 = \left[K_{x1}\sin(x_t x) + K_{x2}\cos(x_t x)\right] A_{2n} e^{e_{tn}t_0} + z_{1t} b_{02}\left[K_{d1}\sin(x_t x) + K_{d2}\cos(x_t x)\right], \; n = 1,2; \quad \text{(A.66)}$$

$$j_1 = \left[-K_{x1}\cos(x_t x) + K_{x2}\sin(x_t x)\right] j_{tn} A_{1n} e^{e_{tn}t_0} + z_{2t} b_{01}\left[-K_{d1}\cos(x_t x) + K_{d2}\sin(x_t x)\right], \quad n = 1,2; \quad \text{(A.67)}$$

$$j_2 = \left[-K_{x1}\cos(x_t x) + K_{x2}\sin(x_t x)\right] j_{tn} A_{2n} e^{e_{tn}t_0} + z_{2t} b_{02}\left[-K_{d1}\cos(x_t x) + K_{d2}\sin(x_t x)\right], \quad n = 1,2; \quad \text{(A.68)}$$

where

$$z_{1t} \equiv -\frac{1}{a}; \quad \text{(A.69)}$$

$$z_{2t} \equiv a\frac{1}{3as_1}x_t \quad \text{(A.70)}$$

.

After redefining various constants, the results can be collected to obtain the following three-scale, two-group approximation to the time-dependent P_1-equations,:

$$f(t) = f_0 + e_1 f_1 + e_2 f_2 =$$
$$[K_{x1}\sin(x_t x) + K_{x2}\cos(x_t x)]\sum_n D_{0n} e^{\frac{b_1}{e_{en}}t_1 + \frac{b_2}{e_{en}}t_2} e^{e_{tn}t_0}$$
$$+ e_1 z_{1t}[K_{d1}\sin(x_t x) + K_{d2}\cos(x_t x)]b_{01} + e_2 z_{1t}[K_{d1}\sin(x_t x) + K_{d2}\cos(x_t x)]b_{02}, \quad n = 1,2; \tag{A.71}$$

$$j(t) = j_0 + e_1 j_1 + e_2 j_2 =$$
$$e_1 z_{2t}[-K_{d1}\cos(x_t x) + K_{d2}\sin(x_t x)]b_{01} + e_2 z_{2t}[-K_{d1}\cos(x_t x) + K_{d2}\sin(x_t x)]b_{02}, \tag{A.72}$$

$$c_1(t) = c_{10} = [K_{x1}\sin(x_t x) + K_{x2}\cos(x_t x)]\sum_n \frac{b_1}{e_{tn}} D_{0n} e^{\frac{b_1}{e_{en}}t_1 + \frac{b_2}{e_{en}}t_2} e^{e_{tn}t_0}$$
$$+ [K_{d1}\sin(x_t x) + K_{d2}\cos(x_t x)]b_{01}, \qquad n = 1,2; \tag{A.73}$$

$$c_2(t) = c_{20} = [K_{x1}\sin(x_t x) + K_{x2}\cos(x_t x)]\sum_n \frac{b_2}{e_{tn}} D_{0n} e^{\frac{b_1}{e_{en}}t_1 + \frac{b_2}{e_{en}}t_2} e^{e_{tn}t_0}$$
$$+ [K_{d1}\sin(x_t x) + K_{d2}\cos(x_t x)]b_{02}, \quad n = 1,2. \tag{A.74}$$

Just as has been shown for the point kinetics equations presented in Section II, the accuracy of numerical computations using the three-scales approximation can be significantly improved by replacing the exponential function for the prompt neutron production term (i.e,. $e^{\frac{b_1}{e_{en}}t_1 + \frac{b_2}{e_{en}}t_2} e^{e_{en}t_0}$) with the exact solution for the equations describing one-group of delayed neutrons, namely $e^{\frac{1}{2}(r-b-e-sq)t_0}$, which is equivalent to effecting the replacement

$$a \equiv \frac{1}{2}(r - b - e - sq), \tag{A.75}$$

in Eqs. A.48 and A.49 for the expressions of b_{01} and b_{02}. The above replacement implies using first-order corrections to the zero-order result. For consistency with this replacement, the variables ε, β and sq need to be redefined by analogy with the one-group of delayed neutrons, as follows:

$$e \equiv \frac{\sum_i l_i b_i}{\sum_i b_i}\Lambda, \tag{A.76}$$

$$b \equiv \sum_i b_i, \tag{A.77}$$

$$sq \equiv \sqrt{a^2 + 2e\,a + e^2 + 4be}\,. \tag{A.78}$$

$$a_m \equiv \frac{b_m}{a + e_m}, \quad m = 1,2. \tag{A.79}$$

The constants D_{0n}, K_{B1}, and K_{B2} are determined by using the initial conditions n_0 and c_{0m}, to obtain

$$D_{02} = -\frac{j_0 c_{c1} - f_0 c_{c1} j_{c3} - c_0 j_{c1} + c_0 j_{c3} - j_0 c_{c3} + f_0 c_{c3} j_{c1}}{c_{c1} j_{c3} + c_{c2} j_{c1} - c_{c2} j_{c3} - c_{c3} j_{c1} - c_{c1} j_{c2} + c_{c3} j_{c2}}, \tag{A.80}$$

$$D_{01} = \frac{j_0 c_{c1} - f_0 c_{c1} j_{c2} - j_0 c_{c2} + f_0 c_{c2} j_{c1} + c_0 j_{c2} - c_0 j_{c1}}{c_{c1} j_{c3} + c_{c2} j_{c1} - c_{c2} j_{c3} - c_{c3} j_{c1} - c_{c1} j_{c2} + c_{c3} j_{c2}}, \quad \text{(A.81)}$$

$$K_{B1} = \frac{\left(2(D_{01} + D_{02})\, a\, b_1 - 2a f_0 b_1 - 2e_1 K_{B2} b_1 + K_{B2} a e_1 (a_1 + 1) - K_{B2} a e_2 (a_2 + 1) - K_{B2} a\, sr\right)}{\left(2e_1 b_1 - a e_1 (a_1 + 1) + a e_2 (a_2 + 1) - a\, sr\right)}, \quad \text{(A.82)}$$

$$K_{B2} = \frac{\left(e_2 (a_2 + 1) - e_1 (a_1 + 1)\right) c_{01} - sr\, c_{01} - 2c_{02} \dfrac{b_1}{a} e_2}{-2sr}, \quad \text{(A.83)}$$

where the quantities jcn are the roots of the cubic equation

$$\begin{aligned} &\left(3s_1\sqrt{-3a_k s_1} - 3e\sqrt{-3a_k s_1}\right) j_{cn}{}^3 + \\ &\left(3e\, s_1 - 6a_k s_1 + 3e\, a_k - 3s_1 a + 3be + 3ae - 3s_1{}^2\right) j_{cn}{}^2 \\ &+ \left(-2s_1\sqrt{-3a_k s_1} - a_k\sqrt{-3a_k s_1} - a\sqrt{-3a_k s_1} + e\sqrt{-3a_k s_1}\right) j_{cn} + a_k s_1 = 0, \end{aligned} \quad \text{(A.84)}$$

while the quantities c_{cn} are defined as

$$c_{cn} \equiv \frac{3j_{cn}^2\sqrt{-3a_k s_1} - 3j_{cn} a_k - 3j_{cn} a - \sqrt{-3a_k s_1} - 3s_1 j_{cn}}{3e j_{cn}}, \quad n = 1,2,3. \quad \text{(A.85)}$$

The initial conditions can be defined either by steady state values, by values computed during the dynamic calculation, from the last computational time-step, or by using the following standardized values: $f(x,0) = f_0\, f(x);\ f_0 = 1;\ j(x,0) = j_0\, j(x);\ c_m(x,0) = c_{0m} c(x);$

$c_{0m} = b_m / (l_m \Lambda)$ for $(m = 1,2); c_0 = \sum_m c_{0m}$; and $j_0 = -\frac{1}{3}\sqrt{\frac{-3a_k}{s_1}}$ for $a_k < 0$ or

$j_0 = \frac{1}{3}\sqrt{\frac{3a_k}{s_1}}$ for $a_k > 0$.